# COMPARISION OF AVIRIS – NG WITH EO-1 HYPERION DATA FOR MINERAL IDENTIFICATION

Himansi Bhatt[1], Dr. Anil Kumar[2], and Mrs. Richa U Sharma[3]

[1,2,3]Indian Institute of Remote Sensing, 4- Kalidas road, Indian Institute of Remote Sensing, ISRO, Dehradun-248001, India,

Email: himansibhatt@gmail.com, anil@iirs.gov.in, richaupadhyay00z@gmail.com

**KEYWORDS:** EO-1 Hyperion, AVIRIS-NG, Spectral Angle Mapper

**ABSTRACT:** Hyperspectral remote sensing is an emerging tool suited for the detection of target resources. It can distinguish the target resources by narrow spectral features. The hyperspectral sensors are mainly categorized into two types; they are airborne sensors and space-borne sensors. The airborne sensor, AVIRIS-NG and the space-borne sensor which is EO-1 Hyperion are used for the study. The hyperspectral data is preprocessed due to the presence of a noise, zero bands, and water absorption bands. The data preprocessing of EO-1 Hyperion includes bad band removal, across track destriping, and atmospheric corrections. For AVIRIS-NG data, the data preprocessing includes bad band removal which contains noise. After data preprocessing, both the hyperspectral data further proceed to reduce the dimensionality of data with the help of Minimum Noise Fraction (MNF). The pure pixels are selected with the help of Pixel Purity Index (PPI). The endmembers classes were generated by n-Dimensional Visualizer (n-D). Spectral Angle Mapper (SAM) algorithm helps in identification of minerals of AVIRIS-NG and EO-1 Hyperion. The primary objective is to compare the AVIRIS-NG and EO-1 Hyperion for mineral identification. The comparison of AVIRIS-NG and EO-1 Hyperion is mainly done on the basis of the mineral map generated by SAM algorithm. Mineral spectra of AVIRIS-NG interpret better than the EO-1 Hyperion.

1. **INTRODUCTION:** After many successful advances in applying multispectral remote sensing for the study of the Earth's characteristics & processes over the decades, a new data acquisition technology is developed, known as Hyperspectral remote sensing. Advances in sensor technology & user's increasing demand for higher resolution data are leading to the great development of hyperspectral remote sensing (Roberto & Filho, 2000). Hyperspectral sensor provides a unique combination of both spatially & spectrally contiguous images that allow precise identification of minerals. During the past two decades, different types of imaging spectrometer have been built with data collected from aircraft and satellite platforms. It collects & processes across the electromagnetic spectrum information. Hyperspectral remote sensing sensor can be of an airborne as well as space-borne type. Hyperspectral remote sensing can be used in various fields, such as in mining, geology, agriculture, forestry, environmental studies. It is a well-developed technique for the mineral detection & many minerals can be identified on the basis of their unique spectra.

## 2. RESEARCH DATASET & STUDY AREA:

### 2.1 DATASET USED:

**2.1.1 EO-1 Hyperion:** The EO-1 Hyperion satellite is launched on 21st November 2000 by NASA's New Millennium Program. EO-1 Hyperion is the first space-borne Hyperspectral sensor for Earth Observation studies. The EO-1 Hyperion is a Push-broom scanner with high spectral resolution. The EO-1 Hyperion

data provides a high-resolution hyperspectral image having 220 spectral bands with the resolution of 30 meters. The swath width of EO-1 Hyperion is 7.5 Km and bandwidth is 10 nm.

**2.1.2** **AVIRIS-NG:** Hyperspectral data using airborne sensor has been used in the geological society since the early 80's (Kruse, Boardman, & Huntington, 2003). AVIRIS-NG is an airborne hyperspectral sensor. AVIRIS-NG stands for Airborne Visible/Infrared Imaging Spectrometer Next Generation. It represents the present state of the airborne hyperspectral remote sensing (Kruse, 2002). It is having a huge number of spectral bands i.e. 425 bands. The swath width and bandwidth of AVIRIS-NG data are 11 Km and 5 nm respectively.

**2.1.3** **ASD Fieldspac4 Spectroradiometer:** The ASD FieldSpac4 spectroradiometer covers the range of 350 nm to 2500 nm. It has the following three sensors: VNIR – 350-1000 nm, spectral resolution – 3 nm, SWIR1 – 1000-1800 nm, spectral resolution – 10 nm, SWIR2 – 1801-2500 nm, spectral resolution – 10 nm.

## 2.2 STUDY AREA:

**2.2.1** **Location:** The study area is Pur-Banera Belt of the Bhilwara Supergroup, located in southern part of Rajasthan between latitude 25.472472° N and longitude 74.647338° E. The study area is shown in Figure 1.

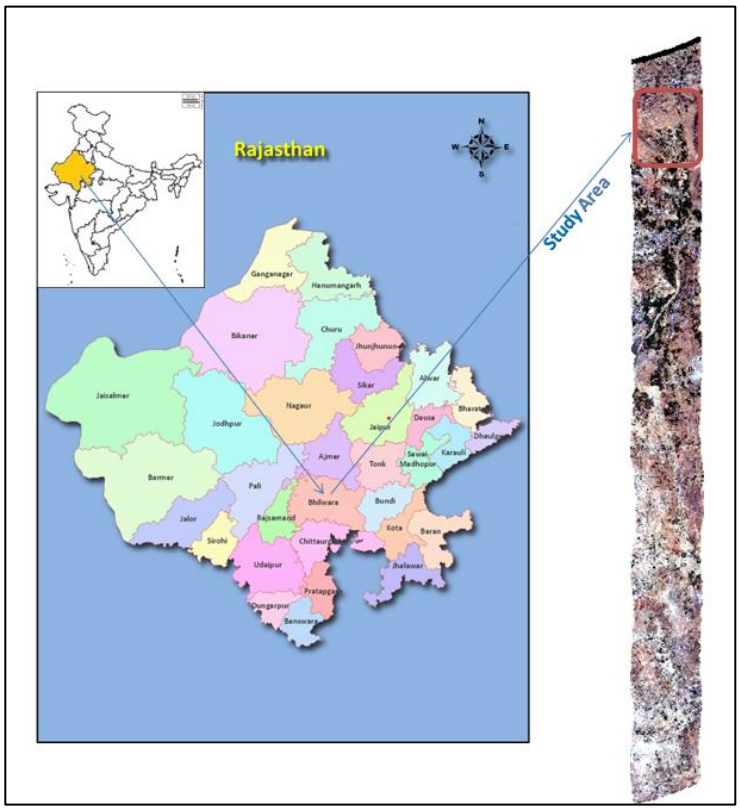


Figure 1: Study Area (Pur-Banera Belt)

**2.2.2 Local Geology:** In Rajasthan, the chain of mountains belongs to the Aravalli Mountains series, which are extended from Delhi (NE) to the Gulf of Cambay (SW). The geological evolution of south-eastern rocks of Rajasthan mainly composed of the Banded-gneiss-complex, Aravalli Supergroup, Delhi Supergroup (Heron, 1953).The mountains mainly consist of Precambrian rocks. The Pur-Banera belt extends over a length of 34 Km having the width of 5 Km. The belt is subdivided into eastern zone and western zone. The eastern zone is consisting of Pb-Zn rich ore whereas western zone consists of Cu-rich ore. Pur-Banera Group is a dominantly chemogenic sequence with bands of metaclastics occurs from south of Banera in the south to Samodi in the north, for over 80 Km in a 3 Km to 12 Km wide belt. These rocks unconformably overlie the rocks of the Potla Formation of the Mangalwar Complex and have been included in the Pur-Banera Group. The unconformity is marked by a polymictic conglomerate coupled with structural break and secular change in the sedimentation pattern. The sequence comprises conglomerate, garnetiferous mica schist, calc-schist, calc-silicate rock, calc-silicate marble, amphibolite, dolomitic marble, magnetite quartzite (a persistent marker horizon) and banded magnetite chert (Shrivastava, 2011). The Pur-Banera Group is of the lower Proterozoic era and is 2500 Ma year old (Ramakrishnan & Vaidyanadhan, 2008). Table 1 represents the stratigraphy of the Pur-Banera group of Bhilwara Supergroup, Rajasthan.

Table 1: Stratigraphy of study area

| Supergroup | Group | Formation | Lithology |
|---|---|---|---|
| Bhilwara Supergroup | Pur-Banera Group | Samodi Formation | Quartzite<br>Mica-Schist<br>Calc-Schist<br>Marble |
| | | Tiranga Formation | Sulphide bearing banded magnetite quartzite |
| | | Rewara Formation | Calc-Gneiss<br>Calc-Schist<br>Mica-Schist<br>Calc Silicate rock<br>Quartzite |
| | | Pur/Pansal Formation | Quartzite<br>Conglomerate |

**2.2.3 Formations of Pur-Banera Formation:**

i. Pur/Pansal Formation: The Pur/Pansal formation mainly comprises of quartzites and conglomerates.

ii. Rewara Formation: In Rewara formation, they are mostly soil covered with scanty exposures. The rock units are calc-schist, calc-gneiss, mica-schist, calc-silicate rocks & quartzite.

iii. Tiranga Formation: The Tiranga Formation is named after the Tiranga hills. The Tiranga formation mainly comprises of sulphide-bearing banded magnetite quartzite.

iv. Saamodi Formation: In the Samodi block the rock unit includes calc-gneiss with calc-schist and quartz-mica schist and marble.

**3. METHODOLOGY:** The AVIRIS-NG dataset is having huge data volume to process. Processing of a strip in a single time is not possible, so subset is created of a desired location. EO-1 Hyperion dataset is also reduced according to the scene of the AVIRIS-NG dataset. Data of **AVIRIS-NG** is of level L2 i.e. radiometrically & atmospherically corrected data. **EO-1 Hyperion** is of L1R type data i.e. radiometrically corrected data, an atmospheric correction of EO-1 Hyperion is required. The large volume of data produced during the hyperspectral image processing which makes handling & computation very difficult. Hence data dimensionality reduction is compulsory and it is done with the help of Minimum Noise Fraction (MNF). The MNF rotation transforms to verify the inherent dimensionality of image information, to separate noise in the data, and to decrease the computational requirements for following processing (Boardman, 1993).Dimensionality reduction performs the transformation of data from a higher dimension to lower dimension without dropping the information. The Pixel Purity Index (PPI) has been widely used for endmember extraction to find most spectrally pure pixels in the MNF image (Boardman, Kruse, & Green, 1995). Spectra of pure pixels are extracted from the n-space with the help of n-dimensional visualize (Boardman & Kruse, 2011). The Spectral Angle Mapper (SAM) algorithm is grounded on an ideal theory that a single pixel of Hyperspectral data denotes one certain material of ground cover, and can be distinctively assigned to one of the ground cover class. The SAM algorithm is based on the measurement of the spectral similarity between two spectra by calculating the spectral angle between them (S, Addamani, Venkat, & S, 2014). Figure 2 represents the working process of Spectral Angle Mapper (SAM).

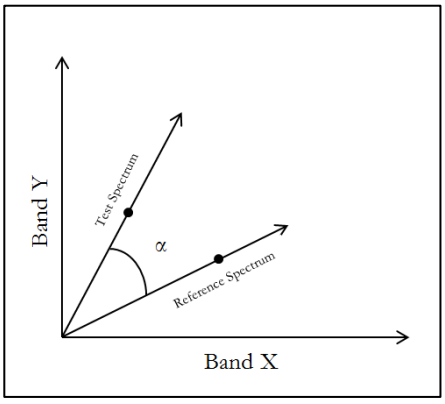


Figure 2: Working process of SAM

The spectral resemblance between an unknown spectra ‘t’ to a reference spectra ‘r’, is expressed in terms of average (spectral) angle ‘α’ between the two spectra which is written in equation 1:

$$\cos\alpha = \left( \frac{\sum_{i=1}^{n} t_i r_i}{\sqrt{\sum_{i=1}^{n} t_i^2 \sum_{i=1}^{n} r_i^2}} \right) \quad (1)$$

**4. RESULTS:** AVIRIS-NG & EO-1 Hyperion datasets identified the minerals which are categorized into three mineral groups. Those mineral groups are of carbonate minerals, clay minerals, and other minerals. Carbonate minerals and Clay minerals are used for the comparison of the both images.

### 4.1 Comparison of AVIRIS-NG and EO-1 Hyperion Mineral Maps:

- The abundance of Carbonate Minerals: The AVIRIS-NG and EO-1 Hyperion classified mineral maps are having carbonate minerals. The carbonate minerals in AVIRIS-NG classified image contain dolomite and calcite whereas in EO-1 Hyperion classified image only dolomite is found. In AVIRIS-NG classified image, dolomite is found in the hilly region which is resembled the geological map of the study area. while in EO-1 Hyperion classified image, dolomite is present in the hilly region as well as in the flat terrain. Hence EO-1 Hyperion misclassified the dolomite mineral.

Figure 3 (A) represents the carbonate minerals in AVIRIS-NG. The yellow circles display the presence of dolomite in the hilly region. Calcite was also found with dolomite. Some traces of chlorite are found with dolomite.

Figure 3 (B) represents the carbonate minerals in EO-1 Hyperion. Dolomite is mapped on hilly and flat terrain as well as in agriculture field. The yellow circles represent the existence of dolomite in the hilly region. The blue circle shows the misclassification of dolomite with vermiculite.

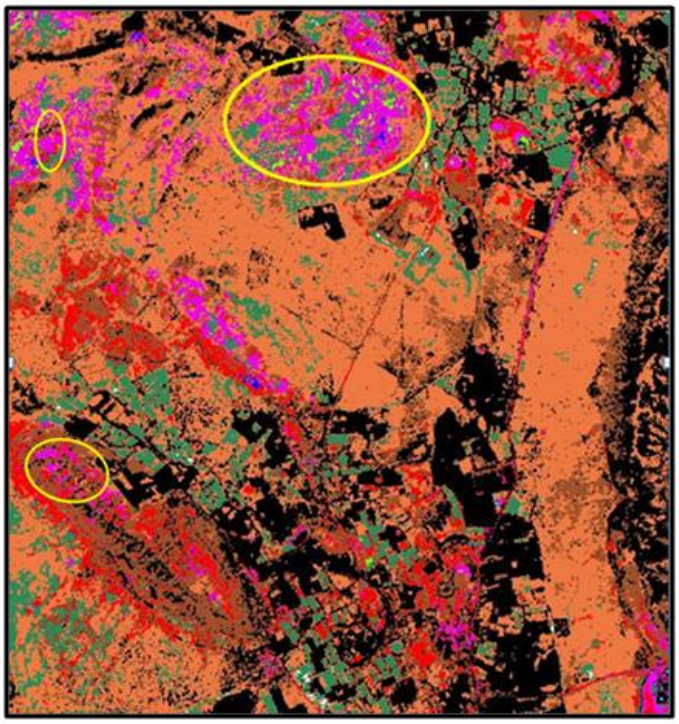

A

**Minerals**

- Montmorillonite
- Calcite
- Augite
- Chlorite
- Dolomite
- Illite
- Nontronite
- Quartz
- Kaosmec#4
- Kaosmec#2

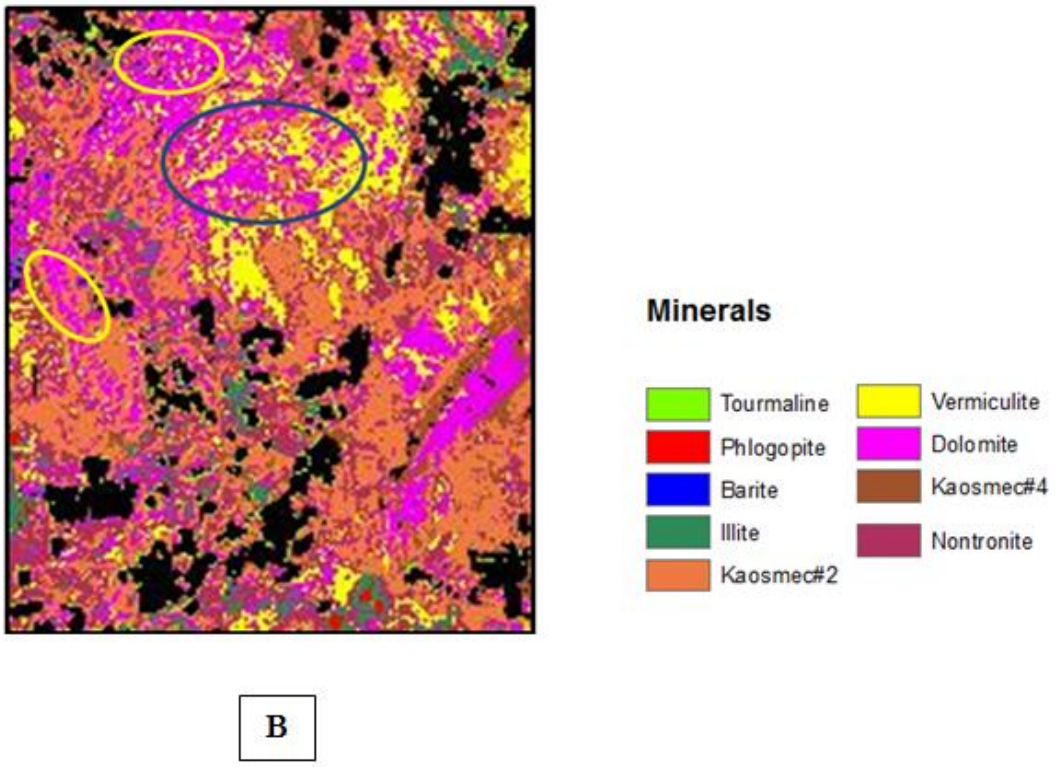


Figure 3: Comparison of Carbonate Minerals. (A) Mineral Map of AVIRIS-NG (B) Mineral Map of EO-1 Hyperion

- The abundance of Clay minerals: The clay minerals found in AVIRIS-NG are montmorillonite, illite, kaolin, nontronite. EO-1 Hyperion is also contained this clay minerals except for montmorillonite. The clay mineral, illite is mainly found in the agricultural field in both AVIRIS-NG and EO-1 Hyperion classified image. Illite contains high potassium which is used with fertilizer for the growth of plants so agriculture fields majorly defined by the illite mineral. EO-1 Hyperion classified image is comparatively poor than the AVIRIS-NG due to intermixing of the nontronite clay with illite. Traces of nontronite are found in AVIRIS-NG classified image whereas, in EO-1 Hyperion, nontronite is misclassified with illite. A mixture of kaolin and smectite are found in both AVIRIS-NG and EO-1 Hyperion classified images. The clay mixture is mainly found in hilly and flat terrain in both of the classified images but in EO-1 Hyperion, the clay minerals of flat terrain are comparatively less due to misclassification of the dolomite and vermiculite minerals.

Figure 4 (A) is illustrating the abundance of clay minerals in AVIRIS-NG. The clay minerals are formed due to weathering of aluminium silicate rocks. The black circle represents the presence of montmorillonite in the field. The yellow circle represents illite clay in the field which is having the characteristic feature of non-expansion. The purple circle represents the presence of a mixture of kaolin with smectite. Mainly kaolin clay is produced by the chemical weathering of feldspar mineral.

Figure 4 (B) is representing the clay minerals in EO-1 Hyperion. The yellow circle represents the illite in agricultural field with dolomite. The blue circles represent kaolin and smectite with dolomite. Due to misclassification presence of dolomite is occurred in illite, kaolin & smectite.

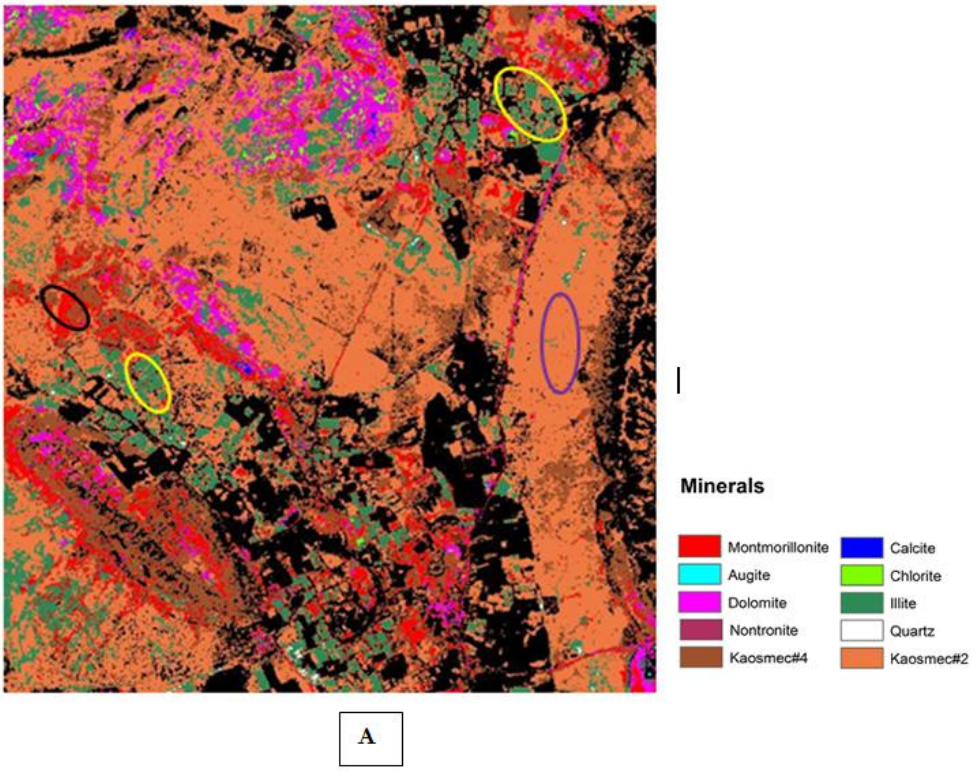


Figure 4: Comparison of Clay Minerals. (A) AVIRIS-NG and (B) EO-1 Hyperion

5. **CONCLUSION:** The key objective of this study is the comparison of AVIRIS-NG with EO-1 Hyperion for identification of the mineral. Comparison of AVIRIS-NG and EO-1 Hyperion is mainly done on the basis of SAM. The SAM classified map of AVIRIS-NG shows better results as compared to a classified map of EO-1 Hyperion. The EO-1 Hyperion has misclassified mainly dolomite with kaolin/smectite and vermiculite while AVIRIS-NG has classified dolomite in hilly regions which resembles the geological map of the study area. In

AVIRIS-NG, illite is classified in agriculture field of the study area as illite is non-expanding clay minerals which are used with fertilizers while in EO-1 Hyperion, illite is also found in agriculture filed but it is misclassified with the dolomite. Misclassification is mainly happened due to the resolution of image i.e. 30 meters.

**References:**


Boardman, J. W. (1993). Automating spectral unmixing of AVIRIS data using convex geometry concepts. In *JPL, Summaries of the 4th Annual JPL Airborne Geoscience Workshop. Volume 1: AVIRIS Workshop* (pp. 11–14). United States: JPL Publication. Retrieved from https://ntrs.nasa.gov/search.jsp?R=19950017428

Boardman, J. W., & Kruse, F. A. (2011). Analysis of imaging spectrometer data using N -dimensional geometry and a mixture-tuned matched filtering approach. *IEEE Transactions on Geoscience and Remote Sensing*, *49*(11), 4138–4152. https://doi.org/10.1109/TGRS.2011.2161585

Boardman, J. W., Kruse, F. A., & Green, R. O. (1995). Mapping target signatures via partial unmixing of AVIRIS data. In *Summaries of the Fifth Annual JPL Airborne Earth Science Workshop. Volume 1: AVIRIS Workshop* (pp. 23–26). United States: JPL Publication. Retrieved from https://ntrs.nasa.gov/search.jsp?R=19950027316

Heron, A. M. (1953). Geology of the Central Rajasthan. *Memoir of the Geological Survey of India*, *79*, 1–389.

Kruse, F. A. (2002). Comparison of AVIRIS and Hyperion for Hyperspectral Mineral Mapping **. In *Proceedings of the 11th JPL Airborne Geoscience Workshop,*. JPL Publication.

Kruse, F. A., Boardman, J. W., & Huntington, J. F. (2003). Comparison of Airborne Hyperspectral Data and EO-1 Hyperion for Mineral Mapping. *IEEE Transactions on Geoscience and Remote Sensing*, *41*(6), 1388–1400. https://doi.org/10.1109/TGRS.2003.812908

Ramakrishnan, M., & Vaidyanadhan, R. (2008). Geology of India. *Geological Society of India*, *1*, 556.

Roberto, C., & Filho, D. E. S. (2000). Hyperspectral Remote Sensing for Mineral Mapping : a Case-Study At Alto Paraíso De Goías , Central Brazil, *30*(3), 551–554.

S, R., Addamani, S., Venkat, & S, R. (2014). Spectral Angle Mapper Algorithm for Remote Sensing Image Classification. *International Journal of Innovative Science, Engineering & Technology*, *1*(4), 201–205. Retrieved from www.ijiset.com

Shrivastava, P. (2011). *Geology and Mineral Resources of Rajasthan*. (P. Gupta & G. Malhotra, Eds.) (3rd Revised, Vol. 30). Jaipur: Director General, Geological Survey of India, Kolkata.